

Unified moving-boundary model with fluctuations for unstable diffusive growth

Matteo Nicoli

Grupo Interdisciplinar de Sistemas Complejos (GISC), Departamento de Matemáticas, Universidad Carlos III de Madrid, Avenida de la Universidad 30, 28911 Leganés, Spain

Mario Castro

Grupo de Dinámica No Lineal and GISC, Escuela Técnica Superior de Ingeniería (ICAI), Universidad Pontificia Comillas, E-28015 Madrid, Spain

Rodolfo Cuerno

Departamento de Matemáticas and GISC, Universidad Carlos III de Madrid, Avenida de la Universidad 30, 28911 Leganés, Spain
(Received 12 March 2008; revised manuscript received 25 April 2008; published 11 August 2008)

We study a moving-boundary model of nonconserved interface growth that implements the interplay between diffusive matter transport and aggregation kinetics at the interface. Conspicuous examples are found in thin-film production by chemical vapor deposition and electrochemical deposition. The model also incorporates noise terms that account for fluctuations in the diffusive and attachment processes. A small-slope approximation allows us to derive effective interface evolution equations (IEEs) in which parameters are related to those of the full moving-boundary problem. In particular, the form of the linear dispersion relation of the IEE changes drastically for slow or for instantaneous attachment kinetics. In the former case the IEE takes the form of the well-known (noisy) Kuramoto-Sivashinsky equation, showing a morphological instability at short times that evolves into kinetic roughening of the Kardar-Parisi-Zhang (KPZ) class. In the instantaneous kinetics limit, the IEE combines the Mullins-Sekerka linear dispersion relation with a KPZ nonlinearity, and we provide a numerical study of the ensuing dynamics. In all cases, the long preasymptotic transients can account for the experimental difficulties in observing KPZ scaling. We also compare our results with relevant data from experiments and discrete models.

DOI: [10.1103/PhysRevE.78.021601](https://doi.org/10.1103/PhysRevE.78.021601)

PACS number(s): 81.10.-h, 68.35.Ct, 64.60.Ht, 81.15.Gh

I. INTRODUCTION

Ever since the beginning of the 19th century [1–3], diffusion-limited growth has attracted the attention of physicists due to its experimental ubiquity and, partly, because it is amenable to continuum descriptions that are sometimes solvable. For instance, electrochemical deposition (ECD) of metals [4,5] has been and still is [6–8] a subject of intense study during this time due to its (in principle) experimental simplicity and its many technological applications: A deposit grows on the cathode when a potential difference is set between two metallic electrodes in a salt solution (generally of Cu, Ag, or Zn). Another interesting system of a conceptually similar type is chemical vapor deposition (CVD) [9], in which a deposit grows from a vapor phase through the incorporation of a reacting species which attaches via chemical reactions once it reaches the aggregate. CVD is one of the techniques of choice for the fabrication of many microelectronic devices and is currently the object of intense study [10–12], partly motivated by its use also in emerging fields of science and technology, such as microfluidics [13]. The practical relevance of ECD and CVD [4,5,9] perhaps makes them appear as two paradigmatic examples of a larger class of growth systems (which will be referred to henceforth as *diffusive*) in which dynamics is a result of the competition between diffusive transport and attachment kinetics at the aggregate interface. Given that growth dynamics in these processes is not constrained in principle by mass conservation, they provide important examples of nonconserved growth [14].

Despite the great amount of work devoted to these systems, they still pose important challenges to a detailed understanding of the very different structures grown under diverse conditions, whose geometries range from fractal to columnar. Partial progress has been achieved so far through the study of the time evolution of the aggregate surface and its roughness [14,15]. In particular, a very successful theoretical framework for such a type of study has been the use of stochastic growth equations for the interface height. Thus, e.g., the celebrated Kardar-Parisi-Zhang (KPZ) equation [16]

$$\frac{\partial h}{\partial t} = V + \nu \nabla^2 h + \frac{V}{2} (\nabla h)^2 + \eta(\mathbf{r}, t) \quad (1)$$

has been postulated as a universal model of nonconserved rough interface growth. In (1), ν is a *positive* constant, $\eta(\mathbf{r}, t)$ is an uncorrelated Gaussian noise representing fluctuations—e.g., in a flux of depositing particles—and V is the average surface growth velocity. Many times the KPZ equation has been put forward as a description of specific experimental growth systems based on symmetry considerations and universality arguments. In view of the fact [17] that very few experiments have been reported which are compatible with the predictions of the KPZ equation (two examples in ECD and CVD are provided in [18,19]), the main drawback of such a theoretical approach [17] is that, in most cases, this coarse-grained level of description does not allow one to make a connection between the experimental and the theoretical parameters, so that it is difficult to assess the cause of

the disagreement between theoretical description and experimental observations. Moreover, such an approach does not allow one to include in a systematic way other potentially important physical mechanisms, such as, e.g., nonlocal effects (typical of diffusive systems) or fluctuations related to mass transport within the dilute phase.

In previous work [20,21] we have put forward an argument as to why many experiments on nonconserved interface growth, such as by ECD and CVD, rarely reproduce the KPZ roughness exponents. Namely, morphological instabilities usually occur in these and many other growth systems that induce long crossovers, making the asymptotic KPZ behavior hard to observe. In this paper, we substantiate further such an approach to the problem of nonconserved growth by constructing a model that incorporates the main constitutive laws common to diffusive growth systems, from which an effective stochastic growth equation can be explicitly derived from first principles.

The aim of this work is threefold: First, our basic (stochastic) moving-boundary problem can be explicitly related to realistic CVD and (simplified) ECD systems. We thus provide a unified picture of these two growth techniques that makes explicit their common features. Nevertheless, due to the generality of the basic constitutive laws that we assume, we expect our model to have implications also for different growth procedures that can be described as *diffusive* in the sense described above. Second, we will use the model equations in order to show why KPZ scaling has been scarcely seen in experiments despite its asymptotic universal validity for nonconserved interface growth. Moreover, we benefit from the model formulation in terms of constitutive laws in order to derive the dependence of coefficients of the effective interface equation with physical parameters. This result seems to be new in the context of diffusive growth and will allow us to show that the form (and properties) of the effective height equation depends crucially on the efficiency of attachment kinetics. Specifically, if the kinetics at the surface is instantaneous—i.e., if the particles aggregate with probability close to unity when they arrive at the surface—the system can be described by an equation which is morphologically unstable, but that still provides non-KPZ scale invariance of the interface fluctuations at large scales. This result reinforces our previous conclusions [20,21] on the experimental irrelevance of KPZ scaling in diffusive growth systems. On the other hand, for slow interface kinetics the effective evolution equation is the well-known (stochastic) Kuramoto-Sivashinsky equation [22], which displays a qualitatively similar dynamics, albeit with a long-scale behavior that does fall into the KPZ class [23–25]. Third, we will interpret some results from experiments and discrete models in light of our continuum theory both qualitatively and quantitatively, a further advance in our understanding of growth dynamics in diffusive systems. As (the deterministic limit of) our model has been profusely tested in the case of CVD, we will mostly consider experiments and models in the ECD context.

The paper is organized as follows. We describe in Sec. II our moving-boundary formulation of diffusive growth systems, including noise terms related to fluctuations in diffusive currents and relaxation events. Section III reports a lin-

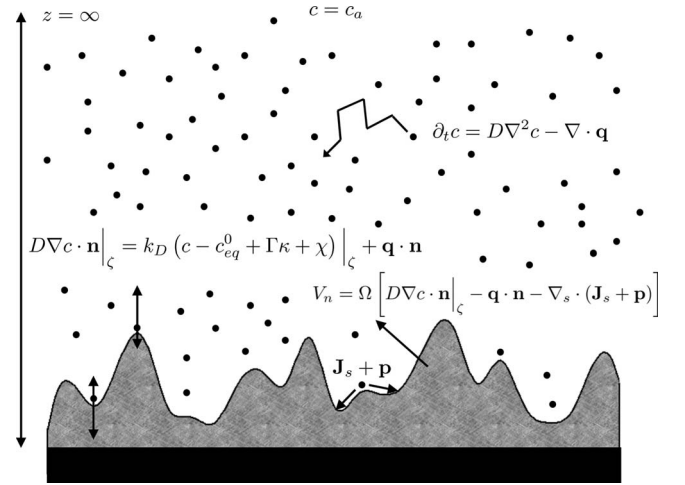


FIG. 1. Schematic representation of a model CVD growth system. Black points represent aggregating units diffusing in the dilute phase. The different transport mechanisms (bulk diffusion, attachment, and surface diffusion) are indicated in the figure by their corresponding equations. See text for definitions and notation; specifically for the noise terms (\mathbf{q} , \mathbf{p} , χ), see Sec. II C.

ear stability analysis of the ensuing unified model of ECD and CVD. Using a small-slope approximation, we derive in Sec. IV a universal nonlinear stochastic equation for the aggregate surface that is numerically studied in the case of infinitely fast kinetics. Section V is devoted to making a connection with several experiments and discrete models on diffusive growth systems. Finally, we conclude in Sec. VI with a discussion of our results, which will allow us to suggest a reasonably approximate picture of nonconserved growth. Some technical details are given in the appendixes.

II. MOVING BOUNDARY PROBLEM

As it turns out, our description of diffusive growth systems takes a form whose deterministic limit has been long studied in the context of CVD. Thus, we first review the classic constitutive equations of CVD [26–28] and subsequently consider the effect of noise due to the fluctuations related to the different relaxation mechanisms involved. Then, we write the equations of ECD growth in a form that unifies this technique with CVD.

A. Chemical vapor deposition

A stagnant diffusion layer of infinite vertical extent is assumed to exist above the substrate upon which an aggregate will grow; see the sketch in Fig. 1. The stagnant layer (typically of the order of cm) is much larger than the typical thickness of the deposit (in the range of microns). The particles within the vapor diffuse randomly until they arrive at the surface, react, and aggregate to it. The concentration of these particles, $c(x, z, t) \equiv c(\mathbf{r}, t)$, obeys the diffusion equation

$$\partial_t c = D \nabla^2 c. \quad (2)$$

In the experiments, the mean concentration at the top of the stagnant layer is chosen to be a constant, equal to the initial average concentration c_a .

Besides this, mass is conserved at the aggregate surface, so the local normal velocity at an arbitrary point on the surface is given by

$$V_n = \Omega D \nabla c \cdot \mathbf{n} - \Omega \nabla_s \cdot \mathbf{J}_s, \quad (3)$$

where Ω is the molar volume of the aggregate and \mathbf{n} is the local unit normal, exterior to the aggregate. The last equation expresses the fact that growth takes place along the local normal direction (usually referred to as *conformal growth* in the CVD literature) and is due to the arrival of particles from the vapor [the first term in Eq. (3)] and via surface diffusion (\mathbf{J}_s stands for the diffusing particle current over the aggregate surface and ∇_s is the surface gradient).

Moreover, the particle concentration c and its gradient at the surface are related through the mixed boundary condition

$$k_D (c - c_{eq}^0 + \Gamma \kappa)|_{\zeta(x,t)} = D \nabla c \cdot \mathbf{n}|_{\zeta(x,t)} \equiv D \partial_n c, \quad (4)$$

where c_{eq}^0 is the local equilibrium concentration of a flat interface in contact with its vapor and $\zeta(x,t)$ is the local surface height. This equation is closely related to the probability of a particle to stick to the surface when it reaches it (see below).

In summary, Eqs. (2) and (3) describe diffusive transport in the vapor phase and the way that particles attach to the growing aggregate. Let us concentrate on the physical meaning of Eq. (4). The parameter Γ is related to temperature [29,30] as $\Gamma = \gamma c_{eq}^0 \Omega / (k_B T)$, where γ is the surface tension (which will be assumed a constant) and $\kappa = (\partial_{xx} \zeta) [1 + (\partial_x \zeta)^2]^{-3/2}$ is the surface curvature. The boundary condition (4) can be obtained analytically, e.g., from kinetic theory by computing the probability distribution for a random walker close to a partially absorbing boundary. There, the particles have a sticking probability s of aggregating irreversibly (i.e., attachment is not deterministic). In such a case [27,31],

$$k_D = \frac{s}{2-s} D L_{mfp}^{-1}, \quad (5)$$

where L_{mfp} is the particle mean free path. Assuming that L_{mfp} is sufficiently small we find two limits in Eq. (5): If the sticking probability vanishes ($s=0$), then $\nabla c=0$ at the boundary, so the aggregate does not grow. On the contrary, if the sticking probability is close to unity (provided L_{mfp} is small enough), then k_D takes very large values and Eq. (4) reduces to the well-known Gibbs-Thomson relation [29,30], which incorporates into the equations the fact that concentration is different in regions with different curvature. In summary, Eq. (4) gives a simple macroscopic interpretation of a microscopic parameter, the sticking probability, and allows us to quantify the efficiency of the chemical reactions leading to species attachment at the interface.

B. Electrochemical deposition

In an electrochemical experiment, dynamics is more complex than in the CVD system as represented above, due to the existence of two different species subject to transport (anions and cations) [32] and an imposed electric field. For a

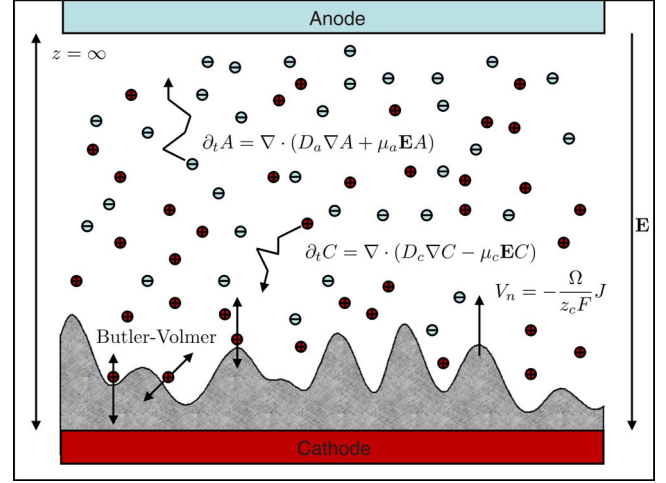


FIG. 2. (Color online) Schematic representation of a model ECD growth system. Cations migrate towards the cathode (lower side) while anions migrate towards the anode (upper side) in an infinite cell. The different transport mechanisms (bulk diffusion and drift, cation reduction) are indicated in the figure by their corresponding equations.

visual reference, see Fig. 2. Although more elaborate treatments of these can be performed [33–35], qualitatively the morphological results are similar to the more simplified description we will be making in what follows. The virtues of the latter include an explicit mapping to the CVD system and explicit experimental verification.

Thus, in ECD, mass transport is not only due to diffusion in the dilute phase, but also due to electromigration and convection. Let C and A be the concentration of cations and anions, respectively; then,

$$\partial_t C = -\nabla \cdot \mathbf{J}_c = \nabla \cdot (D_c \nabla C - \mu_c \mathbf{E} C - \mathbf{v} C), \quad (6)$$

$$\partial_t A = -\nabla \cdot \mathbf{J}_a = \nabla \cdot (D_a \nabla A + \mu_a \mathbf{E} A - \mathbf{v} A), \quad (7)$$

where $D_{c,a}$ are, respectively, the cationic and anionic diffusion coefficients, $\mu_{c,a}$ are their mobilities, and \mathbf{E} is the electric field through the cell, which obeys the Poisson equation

$$\nabla \cdot \mathbf{E} = -\nabla^2 \phi = e N_A (z_c C - z_a A) / \epsilon, \quad (8)$$

with N_A the Avogadro constant, $e z_c$ and $-e z_a$ being the cationic and anionic charges, respectively, ϕ the electric potential, and ϵ the fluid permittivity. The velocity \mathbf{v} of the fluid obeys the Navier-Stokes equation, although we will assume this velocity to vanish in very thin cells [36].

Another interesting experimental variable is the electric current density J , given by

$$J = F (z_c \mu_c C + z_a \mu_a A) E = \sigma(t) E, \quad (9)$$

where $\sigma(t)$ is the apparent electric conductivity. Many experiments exploit the capability of tuning several parameters while maintaining J constant (galvanostatic conditions), hence the relevance of this parameter.

In order to better understand the way in which the particles evolve in the cell, we need to follow their dynamics when the external electric field is switched on. Thus, the

cation and anion concentrations are initially constant and uniform across the cell, and then, once the electric field is applied, anions move towards the anode and cations move towards the cathode. Cations reduce at the cathode, thus forming an aggregate of neutral particles. On the contrary, anions do not aggregate; rather, they merely pile up at the anode, which is dissolving at the same rate as the cations aggregate in the cathode. Hence, the number of cations remains a constant.

Mathematically, this mechanism of aggregation can be expressed as a boundary condition for the cation concentration. Before introducing such a boundary condition we will simplify the set of diffusion equations (6) and (7) following Refs. [37,38]. Let us consider that the deposit moves with a given constant velocity V in such a way that, in the frame of reference comoving with the surface, $z=0$ is the position of the mean height and $z \rightarrow \infty$ represents the position of the anode (thus, we are dealing with the case in which the height of the aggregate is negligible with respect to the electrode separation). Moreover, we will assume that the system is under galvanostatic conditions—namely, that the current density at the cathode, J , is maintained constant. Thus, the problem can be separated into two spatial regions: far enough from and close to the cathode.

At distances larger than the typical diffusion length, $l_D = D/V$, the net charge is zero, so that $z_a A = z_c C$. Hence, multiplying Eq. (6) by $z_c \mu_a$ and adding Eq. (7) multiplied by $z_a \mu_c$, we have

$$\partial_t C = D \nabla^2 C, \quad \partial_t A = D \nabla^2 A. \quad (10)$$

In both equations we have used the ambipolar diffusion coefficient, given by

$$D = \frac{\mu_c D_a + \mu_a D_c}{\mu_a + \mu_c}. \quad (11)$$

Hence, mass transport reduces to a single-variable diffusion equation. It is also important that the electroneutrality condition ($z_a A = z_c C$) implies that the mean interface velocity is equal to the anion migration velocity—that is, $V = \mu_a E_\infty$, where E_∞ is the electric field very far from the cathode (see Refs. [37,38] for further details)—and then

$$\frac{J}{F} = z_c \mathbf{J}_c - z_a \mathbf{J}_a = - \frac{V F z_c C_a}{1 - t_c}, \quad (12)$$

where $t_c = \mu_c / (\mu_a + \mu_c)$ and C_a is the initial cation concentration. Finally, we must provide an equation to describe cation attachment. As a point of departure we will take a relation between the charge transport through the interface and its local properties, given by the well-known Butler-Volmer (BV) equation [4,5,33,39]

$$J = J_0 [e^{(1-b)\eta z_c F/RT} - e^{-(b\eta + \eta_s) z_c F/RT} C_\zeta / C_a], \quad (13)$$

where J_0 is the exchange current density in equilibrium, b is a coefficient which ranges from 0 to 1 and estimates the asymmetry of the energy barrier related to the cation reduction reaction, and $\eta = \Delta\phi - \Delta\phi_{eq}$ is the overpotential, from which a surface curvature contribution η_s has been singled out, of the form

$$\frac{z_c F \eta_s}{RT} = \frac{\Omega \gamma}{RT} \kappa = \Gamma \Omega \kappa, \quad (14)$$

where we have defined the parameter $\Gamma = \gamma/RT$ in the ECD context. The first term on the right-hand side of Eq. (13) is proportional to the rate of the backward reaction, $X \rightarrow X^{n+} + ne^-$, and the second one is proportional to the rate of the forward reaction, $X^{n+} + ne^- \rightarrow X$. The factor C_ζ (the concentration at the surface) is due to the supply of cations at the surface. Since the flux of anions through the cathode is zero (because they neither react nor aggregate), the electric current density at the aggregate surface is only due to the cations and the charge current is proportional to the cation current. Hence [4,40],

$$J = - \frac{z_c D_c F V}{1 - t_c} \nabla C \cdot \mathbf{n} \Big|_\zeta. \quad (15)$$

This equation, combined with Eq. (13), provides a mixed-boundary condition which relates the cation concentration at the boundary with its gradient. In order to cast it into a shape that recalls the CVD relation, we define

$$K_D = \frac{J_0}{z_c F C_a} e^{-b z_c F \eta / RT}, \quad (16)$$

$$C_{eq}^0 = C_a e^{z_c F \eta / RT}, \quad (17)$$

and obtain from (13) and (15)

$$\frac{D_c}{1 - t_c} \nabla C \cdot \mathbf{n} \Big|_\zeta = K_D (C - C_{eq}^0) \Big|_\zeta. \quad (18)$$

The coefficient K_D is related with the sticking probability for cations: if the aggregation is very effective (large sticking probability), the overpotential is a large negative quantity and then K_D grows exponentially. In addition, the concentration C_{eq}^0 decreases. Hence, we can approximate Eq. (18) by $C \approx C_{eq}^0$. In the limit when every particle which arrives at the surface sticks irreversibly, the solution cannot supply enough particles, $C=0$, and the current density takes its maximum value. This value of the current is called the limiting current density. On the other hand, if the sticking probability is small, the system is always close to equilibrium and $\nabla C \approx 0$, so that the net current is zero.

Finally, we close the system with an equation for mass conservation at the boundary. Note that the local velocity of the aggregate surface is proportional to the flux of particles arriving to it; therefore,

$$V_n = - \Omega \mathbf{J}_c \cdot \mathbf{n} = - \frac{\Omega}{z_c F} J, \quad (19)$$

where Ω is the molar volume, here defined as the ratio of the metal molar mass M and the aggregate mean density ρ . For a flat front, $V_n = V$; hence, comparing this equation with Eq. (15) we find

$$\Omega = \frac{M}{\rho} = \frac{1-t_c}{C_a}, \quad (20)$$

a relationship which has been previously proposed theoretically [40] and experimentally verified [36], thus supporting the hypotheses made in this section.

Surely, the reader has noticed that the last equations resemble those for CVD. To emphasize this similarity, we define new variables and parameters as

$$c = R_c C, \quad c_a = R_c C_a, \quad c_{eq}^0 = R_c C_{eq}^0, \quad k_D = \frac{K_D}{R_c}, \quad (21)$$

where $R_c \equiv D_c/[D(1-t_c)]$. With these definitions, Eqs. (2)–(4) describe (under the physical assumptions made above) the evolution of both diffusive growth systems, CVD and ECD.

C. Role of fluctuations

The set of equations presented in the previous section describes the evolution of the mean value of the concentration so that, formally, we can track the position of the interface at any instant. However, it explicitly ignores the (thermal) fluctuations related to the different transport and relaxation mechanisms involved. In order to account for these, we define the stochastic functions \mathbf{q} , \mathbf{p} , and χ as the fluctuations in the flux of particles in the dilute phase ($-D\nabla c$), in the surface-diffusing particle current (\mathbf{J}_s), and in the equilibrium concentration value at the interface, respectively. We choose these noise terms \mathbf{q} , \mathbf{p} , and χ to have zero mean value and correlations given by

$$\langle q_i(\mathbf{r}, t) q_j(\mathbf{r}', t') \rangle = Q \delta_{ij} \delta(\mathbf{r} - \mathbf{r}') \delta(t - t'), \quad (22)$$

$$\langle p_i(\mathbf{r}, t) p_j(\mathbf{r}', t') \rangle = P \delta_{ij} \frac{\delta(\mathbf{r} - \mathbf{r}') \delta(t - t')}{\sqrt{1 + (\partial_x \xi)^2}}, \quad (23)$$

$$\langle \chi(\mathbf{r}, t) \chi(\mathbf{r}', t') \rangle = I \frac{\delta(\mathbf{r} - \mathbf{r}') \delta(t - t')}{\sqrt{1 + (\partial_x \xi)^2}}, \quad (24)$$

where i and j denote vector components and Q , P , and I will be determined from the equilibrium fluctuations following [41,42]. Finally, the factor $\sqrt{1 + (\partial_x \xi)^2}$ in (23) and (24) ensures that the noise strength is independent of the surface orientation.

Thus, the stochastic moving-boundary problem we propose to describe diffusive growth has the form

$$\partial_t c = D \nabla^2 c - \nabla \cdot \mathbf{q}, \quad (25)$$

$$D \partial_n c = k_D (c - c_{eq}^0 + \Gamma \kappa + \chi)|_\zeta + \mathbf{q} \cdot \mathbf{n}, \quad (26)$$

$$V_n = \Omega [D \partial_n c - \nabla_s \cdot \mathbf{J}_s - \mathbf{q} \cdot \mathbf{n} - \nabla_s \cdot \mathbf{p}], \quad (27)$$

$$\lim_{z \rightarrow \infty} c(x, z; t) = c_a. \quad (28)$$

In (27) the surface diffusion term $\nabla_s \cdot \mathbf{J}_s$ is proportional to the surface diffusion coefficient D_s and the surface concentration

of particles, ν_s ; moreover, this term is related to the local surface curvature [29,30]

$$\nabla_s \cdot \mathbf{J}_s = B \nabla_s^2 \kappa,$$

where

$$B = \frac{\Omega^2 \gamma \nu_s D_s}{RT}. \quad (29)$$

In order to determine the values of the coefficients Q , P , and I defined in Eqs. (22)–(24), we use a local equilibrium hypothesis [42,43]. To begin with, let us consider an ideal concentration c_a of randomly distributed particles. The probability of finding n particles in a given volume is given by a Poisson distribution. The mean and variance of this distribution are c_a ; hence, the concentration c satisfies

$$\langle [c(\mathbf{r}, t) - c_a][c(\mathbf{r}', t') - c_a] \rangle = c_a \delta(\mathbf{r} - \mathbf{r}') \delta(t - t'). \quad (30)$$

This equation will allow us to determine Q . First, we write Eq. (25) as

$$\partial_t (c - c_a) = D \nabla^2 (c - c_a) - \nabla \cdot \mathbf{q}. \quad (31)$$

Let $c_{\mathbf{k}\omega}$ and $\mathbf{q}_{\mathbf{k}\omega}$ be the Fourier transforms of $[c(\mathbf{r}, t) - c_a]$ and \mathbf{q} , respectively,

$$c_{\mathbf{k}\omega} = \int dt e^{-i\omega t} \int d\mathbf{r} e^{-i\mathbf{k}\cdot\mathbf{r}} [c(\mathbf{r}, t) - c_a], \quad (32)$$

$$\mathbf{q}_{\mathbf{k}\omega} = \int dt e^{-i\omega t} \int d\mathbf{r} e^{-i\mathbf{k}\cdot\mathbf{r}} \mathbf{q}(\mathbf{r}, t). \quad (33)$$

Writing Eq. (31) in momentum-frequency space and comparing with the Fourier transform of Eq. (30), we find that the spectrum of equilibrium fluctuations is (after integrating out ω)

$$\langle c_{\mathbf{k}} c_{-\mathbf{k}} \rangle = \frac{Q}{2D}. \quad (34)$$

Hence, using (30), we obtain $Q = 2Dc_a$.

Similarly, in order to determine I , we just note that the equilibrium distribution of a curved interface is given by the Boltzmann distribution

$$P(\{\xi\}) \sim \exp\left[-\frac{\mathcal{H}(\{\xi\})}{k_B T}\right], \quad (35)$$

\mathcal{H} being a functional that measures the amount of energy needed to create a perturbation $\xi(x, t)$ about the mean interface height. Moreover, as we are assuming a constant surface tension γ ,

$$\mathcal{H}(\{\xi\}) = \gamma \int_{-L/2}^{L/2} dx [\sqrt{1 + (\partial_x \xi)^2} - 1] \approx \frac{\gamma}{2} \int_{-L/2}^{L/2} dx (\partial_x \xi)^2, \quad (36)$$

provided the perturbation ξ is small enough. The distribution (35) leads to a fluctuation spectrum at equilibrium (for a system with lateral dimension $L \rightarrow \infty$) of the form

$$\langle \zeta_k \zeta_{-k} \rangle = \frac{k_B T}{\gamma k^2}. \quad (37)$$

Introducing the boundary condition (26) into the equation for the velocity, Eq. (27), and linearizing with respect to ζ , we obtain the following algebraic equation in Fourier space:

$$\zeta_{\mathbf{k}\omega} = \frac{\Omega k_D}{i\omega + \Omega k_D \Gamma k^2} \chi_{\mathbf{k}\omega}, \quad (38)$$

where we have neglected the surface diffusion terms. Therefore, integrating $\langle \zeta_{\mathbf{k}\omega} \zeta_{\mathbf{k}'\omega'} \rangle$ in k' and ω' and comparing the ensuing fluctuation spectrum to Eq. (37) we find

$$I = \frac{2\Gamma k_B T}{\Omega k_D \gamma} = \frac{2c_{eq}^0}{k_D}. \quad (39)$$

Finally, in order to calculate P we assume that the fluctuations due to each relaxation mechanism are independent of one another. In this respect, we take the chemical potential difference between the interface and the vapor to be given by [29,30] $\mu = \Omega \frac{\delta \mathcal{H}}{\delta \zeta}$, where $\delta / \delta \zeta$ denotes functional derivative. Linearizing the equation for the velocity and considering only the contribution due to surface diffusion, we get

$$\partial_t \zeta = \frac{\Omega \nu_s D_s}{k_B T} \nabla_s^2 \mu + \eta_{SD} = \frac{\Omega^2 \nu_s D_s}{k_B T} \nabla_s^2 \frac{\delta \mathcal{H}}{\delta \zeta} + \eta_{SD}, \quad (40)$$

where D_s is the surface diffusivity, ν_s is the surface particle concentration, ∇_s^2 is the Laplace-Beltrami (surface) Laplacian and η_{SD} is a noise term related to the fluctuations of the surface diffusion current. To ensure that (35) is the equilibrium distribution, this noise term must satisfy the fluctuation-dissipation theorem [43], which here reads

$$\langle \eta_{SD}(x, t) \eta_{SD}(x', t') \rangle = 2\Omega^2 \nu_s D_s (-\nabla_s^2) \delta(x - x') \delta(t - t'). \quad (41)$$

Therefore, comparing Eq. (40) to Eq. (27) we find that $-\Omega \nabla_s \cdot \mathbf{p} = \eta_{SD}$ and consequently $P = 2D_s \nu_s$.

III. LINEAR STABILITY ANALYSIS

Equations (25)–(28) provide a full description of diffusive growth systems including fluctuations. They thus generalize the classical model of CVD and can also describe (through the appropriate mapping, as seen above) simplified ECD systems. However, such a stochastic moving-boundary problem is very hard to handle for practical purposes. In this section we will reformulate it into an integro-differential form that will allow us to derive (perturbatively) an approximate evolution equation for the interface height fluctuation, $\zeta(x, t)$. In this respect, we will use a technique based on the Green's function theorem which has been successfully applied to other similar diffusion problems [41,42]. For brevity, we show here the main results, leaving the technical details for the interested reader in the appendices.

Our point of departure is the integro-differential equation

$$\begin{aligned} \frac{c(\mathbf{r}, t)}{2} = & c_a - \int_{-\infty}^t dt' \left[\int_{-\infty}^{\infty} dx' \left(V + \frac{\partial \zeta'}{\partial t'} \right) c' G \right. \\ & \left. - D \int_{\zeta'} ds' \left(c' \frac{\partial G}{\partial n'} - G \frac{\partial c'}{\partial n'} \right) \right]_{z'=\zeta'} - \sigma(\mathbf{r}, t), \end{aligned} \quad (42)$$

where G is the Green's function pertinent to the present diffusive problem. The single equation (42) relates the concentration at the boundary with the surface height and is shown in Appendix A to be actually equivalent to the full set of equations (25)–(28), providing essentially the so-called Green's representation formula for our system [44]. Unfortunately, Eq. (42) is still highly nonlinear and has also multiplicative noise (through the noise term σ ; see Appendix A). Notwithstanding, it will allow us to perform a perturbative study in a simpler way.

First, let us consider solutions of Eq. (42) that are of the form $c = c_0 + c_1$, where c_0 stands for the part associated with the flat (i.e., \mathbf{r} -independent) front solution and c_1 is a small perturbation of the same order as the height fluctuation $\zeta(x, t)$. Hence, to lowest order in the latter and its derivatives (see Appendix B),

$$c_0 = \frac{V c_a + k_D c_{eq}^0}{V + k_D}. \quad (43)$$

Thus, the particle concentration at a flat surface is an average between its local equilibrium value c_{eq}^0 and that at the top of the stagnant layer, c_a , weighted by the two characteristic velocities of the moving-boundary problem, V and k_D . One remarkable feature of the Green's function representation is that, from knowledge of the concentration at the boundary, we can extrapolate the value of the particle concentration everywhere. Thus, from Eq. (42) and using (A7) we find

$$c_0(z) = c_a + (c_0 - c_a) e^{-zV/D}. \quad (44)$$

This equation has been theoretically obtained and experimentally verified by Léger *et al.* [40].

We now proceed with the next order of the expansion. At this order we already obtain a proper (albeit linear) evolution equation for the interface, which moreover contains all the noise terms contributions—that is (see Appendix C),

$$\partial_t \zeta_k(t) = \omega_k \zeta_k(t) + \eta_k(t), \quad (45)$$

where ω_k is a function (dispersion relation) of wave vector k whose form may change with the values of the phenomenological parameters (see below) and gives the rate at which a periodic perturbation of the flat profile grows (if $\omega_k > 0$) or decays (if $\omega_k < 0$) as a function of k . Note that, being linear, Eq. (45) can be exactly solved.

It turns out that the behavior of ω_k can be most significantly studied as a function of the values of the kinetic coefficient k_D , as anticipated in Secs. II A and II B. Specifically, we analyze separately the case in which surface kinetics is instantaneous (that is, the sticking probability is high) and all other cases in which the attachment rate is finite.

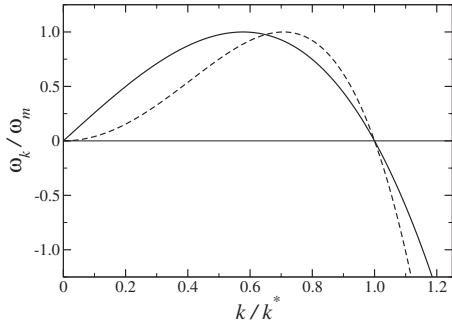


FIG. 3. Linear dispersion relations given by Eqs. (46) (dashed line) and (48) (solid line), normalized by the growth rate of the most unstable mode, vs spatial frequency k normalized by k^* . Both axes are in arbitrary units.

A. Noninstantaneous surface kinetics ($k_D < \infty$)

For a finite value of the kinetic coefficient k_D , we cannot obtain (even in the zero-noise limit) the linear dispersion relation ω_k in a closed analytic form, unless we perform a large-scale ($k \rightarrow 0$) approximation. Thus, we can analyze implicitly the zeros of the function $\mathcal{T}_{k\omega}$ defined in (C5), which yield the required form of ω_k as a function of the wave vector [45]. In the large-scale limit we find [46]

$$\omega_k = a_2 k^2 - a_4 k^4, \quad (46)$$

where

$$a_2 = \frac{Dk_D}{V} \Delta, \quad a_4 = \frac{Dk_D l_D d_0 \Delta}{V \left[1 - \sqrt{\frac{Vd_0}{D}} \right]}, \quad (47)$$

and $\Delta = 1 - d_0/l_D$. The two constants appearing in Δ are the capillarity length ($d_0 \equiv \Gamma\Omega$) and the diffusion length ($l_D \equiv D/V$). If $\Delta < 0$, then $k=0$ is the only zero of ω_k , and since $a_2 < 0$, all Fourier modes $\zeta_k(t)$ of the height fluctuation are stable, since they decay exponentially in time within linear approximation.

On the contrary, if $\Delta > 0$, then a_2 and a_4 are both positive and there is a band of unstable modes for $k \in (0, k^*)$, with $k^* = [\frac{V}{Dd_0} (1 - \sqrt{\frac{Vd_0}{D}})]^{1/2}$. For these values of the wave vector, $\zeta_k(t)$ grows exponentially in time within linear approximation. A maximally unstable mode exists corresponding to the maximum positive value of ω_k , whose amplitude dominates exponentially all other and leads to the formation of a periodic pattern. Under these parameter conditions, the dispersion relation (46) is that of the linear Kuramoto-Sivashinsky (KS) equation (see Fig. 3) [22].

Although the above linear dispersion relation contains $O(k^4)$ terms, typical of relaxation by surface diffusion [29,30], these originate as higher-order contributions in which diffusion (D), aggregation (k_D), and surface tension (Γ) become coupled. We can also include proper surface diffusion into the analysis, for which we simply have to replace a_4 by $a_4 + B\Omega(V + k_D)/V$, with B as in (29), which merely shifts k^* closer to zero. In this case, the band of unstable modes shrinks, which is consistent with the physical smoothing effect of surface-diffusion at short length scales.

B. Instantaneous surface kinetics ($k_D \rightarrow \infty$)

If the sticking probability is essentially 1, as seen above, $k_D \rightarrow \infty$. This fast attachment condition occurs in many irreversible growth processes [47]. Following a similar procedure (and long-wavelength approximation) as the one that led us to the KS dispersion relation in the previous section, we now get

$$\omega_k = D \left(\frac{\Gamma^2 \Omega^2}{2} - \frac{B\Omega}{D} \right) k^4 - \frac{3\Gamma\Omega V k^2}{2} + |k| (V - \Gamma\Omega D k^2) \left[1 - \frac{\Gamma\Omega V}{D} + \left(\frac{\Gamma^2 \Omega^2}{4} - \frac{B\Omega}{D} \right) k^2 \right]^{1/2}.$$

This expression has several interesting limits. For instance, if we neglect surface tension and surface diffusion terms (that is, for $\Gamma=B=0$), then $\omega_k = V|k|$, the well-known dispersion relation of the diffusion-limited-aggregation (DLA) model [47]. In this case, every spatial length scale is unstable, the shortest ones (large k values) growing faster than the larger ones. Thus, in such a case the aggregate consists of wide branches plenty of small tips. Moreover, there is actually no characteristic length scale in the system; hence, the aggregate has scale invariance (that is, it is self-similar).

If we only neglect the surface diffusion term and since d_0 is typically in the range $10^{-7} - 10^{-6}$ cm and l_D is close to $10^{-1} - 10^{-2}$ cm, we can write

$$\omega_k \simeq V|k|(1 - d_0 l_D k^2), \quad (48)$$

which is the celebrated Mullins-Sekerka (MS) dispersion relation [48,49] (see Fig. 3), ubiquitous in growth systems in which diffusive instabilities (induced by shadowing of large branches over smaller surface features) compete with relaxation by surface tension. This dispersion relation has been experimentally verified in several ECD systems [50–52] and has actually been theoretically proposed before for ECD by Barkey *et al.* [53] (although under nongalvanostatic conditions).

However, in many diffusive growth systems both surface tension and surface diffusion are non-negligible; considering again the physical hypothesis $d_0 \ll l_D$ and a long-wavelength approximation, we get

$$\omega_k = V|k| [1 - (d_0 l_D + B\Omega/2D)k^2] - B\Omega k^4. \quad (49)$$

Nevertheless, there are, e.g., some CVD conditions [19,54], for which the vapor pressure in the dilute phase is so low that relaxation by evaporation and condensation is negligible in practice. In such a case, the dispersion relation is provided by (49) with an effective zero value for d_0 .

Finally, quite analogously to the KS case seen above, the last dispersion relations [Eqs. (48) and (49)] show a competition between mechanisms which tend to destabilize the interface and others which tend to stabilize it. From this competition, a characteristic length scale arises, λ_m , which grows exponentially faster than the others ($\lambda_m = 2\pi/k_m$, with k_m being the value for which ω_k is a positive maximum).

In summary, we see that, in reducing the efficiency of attachment from complete ($k_D \rightarrow \infty$) to finite ($k_D < \infty$), the symmetry of the dispersion relation changes so that nonlocal

terms like odd powers of $|k|$ are replaced by local (linear) interactions. For instance, $-k^2\zeta_k(t)$ is the Fourier transform of the local term $\partial_x^2\zeta(x,t)$, while $|k|\zeta_k(t)$ cannot be written as (the transform of) any local differential operator acting on $\zeta(x,t)$. This result can be understood heuristically: if the sticking probability is small, then particles arriving at the interface do not stick to it the first time they reach it, but they can explore other regions of the aggregate. This attenuates the nonlocal shadowing effect mentioned above, so that growth becomes only due to the local geometry of the surface.

Although the $k_D \rightarrow \infty$ limit is a mathematical idealization, for practical purposes we can determine under which conditions it is physically attained. Thus, if we introduce Eq. (44) describing the concentration field for a flat interface into the boundary condition (26), the latter takes the form

$$\frac{c - c_{eq}^0}{D/k_D} = \frac{c - c_0}{D/V}. \quad (50)$$

The term D/V is the diffusion length; hence, analogously, we can define D/k_D as a *sticking length*. Physically, this length can be seen as the typical distance traveled by a particle between its first arrival at the interface and its final sticking site. We can neglect this length scale if the sticking probability is close to unity. On the contrary, if $k_D \rightarrow 0$, the distance that the particle can explore before attaching is infinite. Therefore, taking Eq. (50) into account, we can say that the $k_D \rightarrow \infty$ limit describes accurately the problem for any finite k_D as long as it is much larger than V . In such a case the diffusion length and the capillarity length determine the characteristic length scale of the system.

IV. NONLINEAR EVOLUTION EQUATION

In this section we proceed one step further with our perturbative approach by including the lowest-order nonlinear contributions to Eq. (45). If we evaluate the Green's function of the problem at the boundary we find

$$G(\mathbf{r} - \mathbf{r}', \tau) = \frac{\Theta(\tau)}{4\pi D\tau} \exp\left[-\frac{(x-x')^2}{4D\tau} - \frac{(\zeta - \zeta' + V\tau)^2}{4D\tau}\right], \quad (51)$$

where $\tau = t - t'$. Expanding the last term in the argument of the exponential as a series in ζ we get $(\zeta - \zeta')^2 + 2V(\zeta - \zeta')\tau + V^2\tau^2$. The second and third terms were already taken into account before in the linear analysis, so the only nonlinear contribution in Eq. (51) is related to the first term $(\zeta - \zeta')^2$, which introduces a correcting factor $\exp[-(\zeta - \zeta')^2/(4D\tau)]$ which is only significant when $\zeta' \approx \zeta$; hence, we can replace $\zeta' - \zeta$ by the lowest term in its Taylor expansion to get

$$\exp\left(-\frac{(\zeta - \zeta')^2}{4D\tau}\right) \approx 1 - \frac{(\partial_x\zeta)^2(x' - x)^2}{4D\tau}. \quad (52)$$

By incorporating this contribution into the formulas of Appendixes A–C, the consequence can be readily seen to be the addition of a mere term equal to the (Fourier transform of) $V(\partial_x\zeta)^2/2$ to the right-hand side of Eq. (45), resulting in an evolution equation with the form

$$\partial_t\zeta_k(t) = \omega_k\zeta_k(t) + \frac{V}{2}\mathcal{N}[\zeta]_k + \eta_k(t), \quad (53)$$

where $\mathcal{N}[\zeta]_k$ is the Fourier transform of $\mathcal{N}[\zeta] = (\partial_x\zeta)^2$. Note that the nonlinear term obtained is precisely the characteristic KPZ nonlinearity as in Eq. (1), which appears here with a coefficient equal to half the average growth velocity, agreeing with standard mesoscopic arguments [16]. Moreover, as is well known [14], this is the most relevant nonlinear term (asymptotically) that can be obtained for a nonconservative growth equation such as Eq. (42); hence, any other nonlinear term will not change the long-time, long-scale behavior of the system. As we have shown above, for small sticking ω_k is given by Eq. (46) and for large sticking it is given by Eq. (49). In all cases the noise correlations involve constant terms, as well as terms that are proportional to successively higher powers of k . By retaining only the lowest-order contributions in a long-wavelength and quasistatic approximation, from Eq. (C8) we obtain

$$\langle \eta_{k\omega}\eta_{k'\omega'} \rangle = (\Pi_0 + \Pi_2 k^2)\delta(k+k')\delta(\omega+\omega'), \quad (54)$$

where

$$\Pi_0 = \begin{cases} Vc_0\left(1 + \frac{2V}{k_D}\right), & k_D < \infty, \\ Vc_{eq}^0, & k_D \rightarrow \infty, \end{cases} \quad (55)$$

and

$$\Pi_2 = \begin{cases} 2\Pi_0 l_D^2 + 2D_s\nu_s\left(1 + \frac{V}{k_D}\right)^2, & k_D < \infty, \\ 2\Pi_0 l_D^2 + 2D_s\nu_s, & k_D \rightarrow \infty, \end{cases} \quad (56)$$

where Eq. (43) for c_0 is to be used in the case of finite kinetics. In general, the parameter Π_0 provides the strength of nonconserved noise, while Π_2 measures the contribution of conserved noise [55] to the interface fluctuations.

We can briefly interpret the physical content of Eqs. (55) and (56). Thus, in the case of very high sticking conditions, $k_D \gg V$, aggregate growth is diffusion limited because of the very efficient reaction kinetics, and the variance of nonconserved fluctuations is simply proportional to the particle concentration at the surface. The opposite scenario occurs when the kinetic coefficient is negligible as compared to the mean interface growth velocity, $k_D \ll V$, and the process becomes reaction limited. In this case, the concentration at the interface, c_0 , is proportional to the particle concentration at infinity, c_a , and nonconserved fluctuations are enhanced. Finally, in the case of comparable average velocity and kinetic coefficient, $V \approx k_D$, the reaction kinetics at the surface and the diffusion in the bulk have a similar relevance, Π_0 being proportional to a weighted mean between c_{eq}^0 and c_a .

On the other hand, the variance of the conserved noise, Π_2 , is composed by two terms. The first one arises as a higher-order contribution of the nonconserved noise, in which the typical diffusion length l_D appears. The second one (proportional to $D_s\nu_s$) originates in the conserved mechanism of surface diffusion. The presence of conserved noise can naturally modify some short length and time scales

of the system, but in the presence of nonconserved noise, it is known to be irrelevant to the large-scale behavior. Thus, Π_2 will be neglected in the numerical study performed below.

For the case of finite kinetic coefficient, the evolution equation (53) is the stochastic generalization of the KS equation [23–25]. In the case of fast attachment $k_D \rightarrow \infty$, the resulting interface equation combines the linear dispersion relation of MS with the KPZ nonlinearity. In this sense it employs two “ingredients” that seem ubiquitous in growth systems, so we find remarkable the fact that (to the best of our knowledge) its detailed dynamics has not been reported so far. The purpose of the next section is to report a numerical study of this equation in order to clarify the similarities and differences to its finite attachment counterpart.

A. Numerical results

1. Pseudospectral method

As noted above, although the shape of the nonlinear equation (53) is common to both sticking limits, their dispersion relations make them very different physically. Thus, while the linear terms of the KS equation are local in space, linear terms corresponding to MS dispersion relation cannot be written in terms of local spatial derivatives. Therefore, we cannot perform a standard finite-difference discretization in order to implement its numerical integration [55]. Rather, in order to integrate numerically Eq. (53) we will resort to the so-called pseudospectral methods that make use both of real and Fourier space representations. Such techniques have been successfully used, e.g., in many instances of the physics of fluids [56] and are being used more recently in the study of stochastic partial differential equations [57–61].

As we are interested in the qualitative scaling properties of Eq. (53), rather than, say, in a quantitative comparison to a specific physical system, we introduce positive constants ν , K , B , and λ , which allow us to write the equations in the more general form for each limit:

$$\partial_t \zeta_k(t) = (\nu k^2 - K k^4) \zeta_k + \frac{\lambda}{2} \mathcal{N}[\zeta]_k + \eta_k(t), \quad (57)$$

$$\partial_t \zeta_k(t) = (\nu |k| - K |k|^3) \zeta_k + \frac{\lambda}{2} \mathcal{N}[\zeta]_k + \eta_k(t), \quad (58)$$

where, in order to stress the similarities between the two interface equations, we have neglected in (58) the $O(k^4)$ terms, given that their stabilizing role is already played by the $O(|k|^3)$ term. In what follows, we will only refer to the new parameters, which will later be estimated in the next section when we analyze different experimental conditions.

In order to integrate efficiently Eq. (53) we use a pseudospectral scheme. This numerical method is detailed in [61] and employs an auxiliary change of variable that allows to estimate the updated value of ζ_k as

$$\zeta_k(t + \Delta t) = e^{\omega_k \Delta t} \left(\zeta_k(t) + \frac{\lambda}{2} \Delta t \mathcal{N}[\zeta(t)]_k \right) + r_k(t), \quad (59)$$

where the noise term $r_k(t)$ is conveniently expressed as

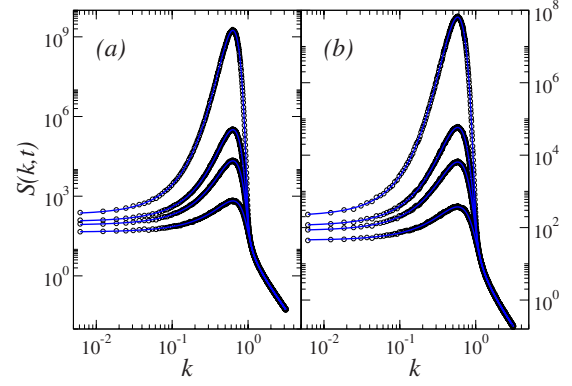


FIG. 4. (Color online) Power spectral density $S(k, t)$ from numerical simulations for a $L=1024$ system with $\nu=K=1$, $\Pi_0=10^{-2}$, and $\lambda=0$ (i.e., linearized equations), averaged over 10^3 realizations, at times $t=4, 8, 10$, and 20 for (a) Eq. (57) (open circles) and (b) Eq. (58) (open circles). Blue solid lines represent the exact solution, Eq. (61), for each case. All axes are in arbitrary units.

$$r_k(t) = \sqrt{(\Pi_0 + \Pi_2 k^2) \frac{e^{2\omega_k \Delta t} - 1}{2\omega_k \Delta x}} v_k(t), \quad (60)$$

with $v_k(t)$ being the Fourier transform of a set of Gaussian random numbers with zero mean and unit variance [58]. Regarding the explicit calculation of the nonlinear term in Eq. (59), we perform the inverse Fourier transform of $-ik\zeta_k$ and take the square of it in real space, so that we explicitly avoid nonlinear discretization issues [57]. However, in this procedure aliasing issues arise [56], which we avoid by extending the number of Fourier modes involved in the integration and using zero padding; see details in [56,57].

2. Numerical integration

As mentioned, the noisy KS equation (57) has been extensively studied in the literature, so we will concentrate in this section on Eq. (58). Its behavior will help us to understand the evolution of the interface in the $k_D \rightarrow \infty$ cases.

The linear regime is very similar for both equations, as one might naively expect. In fact, we find that both systems feature similar power spectral densities (or surface structure factors) $S(k, t) = \langle \zeta_k(t) \zeta_{-k}(t) \rangle$; see Fig. 4. This can be easily understood by inspection of the analytic result for $S(k, t)$ obtained from the exact solution of Eq. (45),

$$S(k, t) = \Pi_0 \frac{e^{2\omega_k t} - 1}{2\omega_k}, \quad (61)$$

where the corresponding dispersion relations are displayed in Fig. 3. By simple inspection of Fig. 4 one is tempted to say that both Eqs. (57) and (58) have a similar behavior so that, *a priori*, KPZ scaling might be expected in the asymptotic regime also for the latter. However, for this fast kinetics equation, we show in Fig. 5 that the growth exponent β characterizing the power-law growth of the surface roughness or global width $W(t) \sim t^\beta$, where $W^2(t) = (1/L^2) \sum_k S(k, t)$ [14,15], is much larger at long times than the expected KPZ value $\beta_{KPZ}=1/3$. A rationale for such a long-time behavior of Eq. (58) can be already provided by

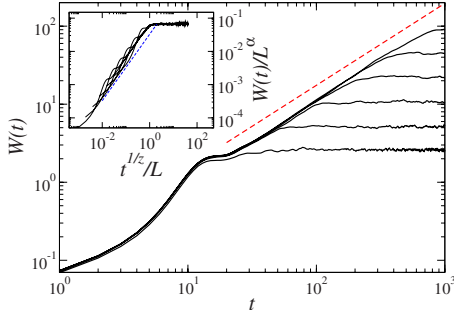


FIG. 5. (Color online) Global width vs time for a system with $\nu=K=\lambda=1$ and $\Pi_0=10^{-2}$ obtained numerically for Eq. (58), for increasing system sizes, $L=32, 64, 128, 256, 512,$ and 1024 , bottom to top, averaged over 10^3 realizations. The red dashed line is a guide to the eye with slope 1.05 suggesting the asymptotic value of β . Inset: collapse of $W(t)$ using $\alpha=1.00, \beta=1.05,$ and $z=0.95$. The blue line has slope 1.00, showing the consistency of our estimate for α . Axes in the main panel and in the inset are all in arbitrary units.

simple dimensional analysis. Thus, under the scale transformation $t \rightarrow b^z t, k \rightarrow b^{-1} k, \zeta_k \rightarrow b^{\alpha+1} \zeta_k$, Eq. (58) becomes

$$\partial_t \zeta_k = b^{z-1} \nu |k| \zeta_k - b^{z-3} K |k|^3 \zeta_k + b^{\alpha+z-2} \frac{\lambda}{2} \mathcal{N}[\zeta]_k + b^{z/2-\alpha-1/2} \eta_k. \tag{62}$$

If we introduce the exact one-dimensional KPZ exponents ($\alpha=1/2, z=3/2$), it is easy to see that in the hydrodynamic limit (that is, when $b \rightarrow \infty$) the most relevant term in the equation is *not* the KPZ term, but rather the lowest-order linear term $|k| \zeta_k$. Preliminary dynamic renormalization-group calculations [62] seem to provide the same result. The present scaling argument provides moreover the exponent values $\alpha=\beta=z=1$ at the stationary state. These values are compatible with those obtained from numerical simulations of Eq. (58), as displayed in Figs. 5 and 6. The numerical values we obtain for the exponents are $\alpha=1.00 \pm 0.05, \beta=1.05 \pm 0.05,$ and $z=0.95 \pm 0.05$; thus, they are in good

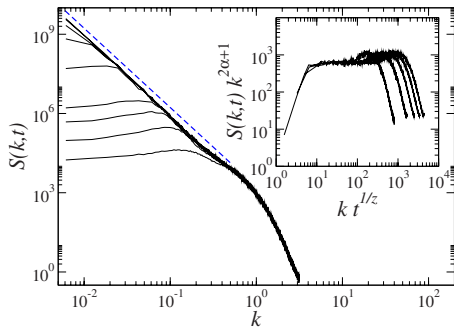


FIG. 6. (Color online) Power spectrum vs spatial frequency k with the same parameters as in Fig. 5 and $L=1024$. Different curves stand for different times (the one at the bottom is for the earliest time). The dashed line is a guide to the eye with slope -3 , compatible with $\alpha=1$. Inset: collapse of $S(k,t)$ using $\alpha=1.00, \beta=1.05,$ and $z=0.95$. Axes in the main panel and in the inset are all in arbitrary units.

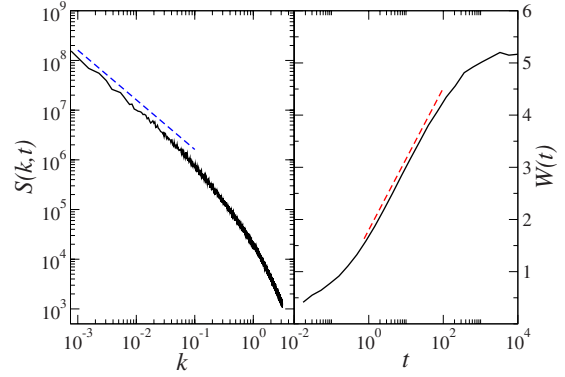


FIG. 7. (Color online) Left: power spectral density vs wave vector for Eq. (58) with $\nu=-1, K=1, \lambda=4, \Pi_0=10, L=8192,$ and averages over 100 noise realizations. The dashed line is a guide to the eye with slope -1 [that is, $\alpha=0$ (log)]. Right: global roughness vs time for the same system as in the left panel. Note the semilogarithmic representation. The dashed line is a guide to the eye representing $W(t) \sim \log t$ before saturation. All axes are in arbitrary units.

agreement with the ones predicted by dimensional analysis. In order to check the consistency of our numerical estimates [63,64], in the inset of Fig. 6 we show the collapse of the power spectrum density using these exponent values. Collapses are satisfactory, including the behavior of the scaling function for the width, indicated by a solid line in the inset of Fig. 5. The discrepancies in the collapsed curves for large $kt^{1/z}$ values are due to the existence of a short-scale scaling different from the asymptotic one.

From our numerical results, we conclude that the nonlinear regime as described by Eq. (58), corresponding to instantaneous kinetics, is very different from that for slow kinetics, as represented by the noisy KS equation. Thus, in both cases the KPZ nonlinearity is able to stabilize the system and induce power-law growth of the surface roughness, associated with kinetic roughening properties. However, the universality class of Eq. (58) is *not* that of the KPZ equation, but rather it is a new class completely determined by the $|k|$ term in the linear dispersion relation. Note moreover that the new exponents associated with the asymptotic regime for this equation fulfill *accidentally* the Galilean scaling relation $\alpha+z=2$ [14,16]. We describe this property as accidental due to the fact that Eq. (58) is *not* Galilean invariant. The easiest way to confirm this is to check for the scaling behavior of a *stable* version of Eq. (58) in which we take *negative* ν values for which all modes are linearly stable. Figure 7 shows in the left panel the power spectral density in this case, which behaves as $S(k) \sim 1/k$ for long distances. Moreover, in the right panel of this figure we plot the time evolution of the global roughness for the same system, which behaves as $W(t) \sim \log t$ for long times before saturation. From these data we conclude the exponent values are $z=1$ and $\alpha=0$ (log), which do *not* satisfy the scaling relation implied by Galilean invariance. Such a stabilized version of Eq. (58) has been studied in the context of diffusion-limited erosion [65].

V. COMPARISON WITH EXPERIMENTS AND DISCRETE MODELS

In this section, we focus on the applications of the model equations to understand and explain some experimental re-

sults, qualitatively and quantitatively, and, besides, compare our results from continuum theory to relevant discrete models of diffusion-limited growth.

A. Experiments

From the experimental point of view, it is very difficult to determine if the dispersion relation characterizing a specific physical system is the MS or, rather, the KS one, because they are both very similar except very near $k=0$ (see Fig. 3). In principle, such a distinction would be very informative, since it could provide a method to assess whether the dynamics is diffusion limited ($k_D \rightarrow \infty$) or else reaction limited ($k_D \ll V$). Several previous theoretical works in this field [66,67] predict, qualitatively, a KS dispersion relation, while others [53] predict a dispersion relation similar to the one of MS. All those studies are not necessarily incompatible with one another because they consider different experimental conditions. Moreover, to our knowledge, there are only a few experimental reports in which the dispersion relation is measured, and in most cases the authors presume that it can be accounted for by MS [50–52]. Notwithstanding, within experimental uncertainties that are specially severe at small wave vectors, they could all equally have been described by the KS dispersion relation.

Another way to distinguish which is the correct effective interface equation that describes a given system could be the value of the characteristic length associated with the most unstable mode that can be measured (which, in fact, would be essentially the characteristic length scale that could be observed macroscopically for the system). Unfortunately, from Eqs. (46) and (48) one has that, for $d_0 \ll l_D$, then $k_m = (2l_D d_0)^{-1/2}$ for the KS and $k_m = (3l_D d_0)^{-1/2}$ for the MS dispersion relations. Hence, except for a constant numerical value of order unity, both cases provide a characteristic length scale that depends equally on physical parameters, while the significant parameter k_D only modifies ω_m —namely, the characteristic time at which the instability appears (which is about ω_m^{-1}). Thus, in order to clarify the nature of the growth regime (diffusion or reaction limited), one should rather study the long-time behavior of the interface.

Despite these difficulties, we can still try to interpret some experimental results reported in the literature. Lèger *et al.* [38,40,68] have presented several exhaustive works dealing with ECD of Cu under galvanostatic conditions. In addition to properties related to the aggregate, they also provide detailed information about the cation concentration. Their main result in this respect is that such a concentration obeys experimentally Eq. (44) as we anticipated above. It can also be seen that the product aggregates are branched and that the topmost site at every position x defines a rough front growing with a constant velocity. In Fig. 8 of Ref. [40] the authors plot the branch width against the diffusion length. From that figure, it is clear that λ_m and l_D are not linearly related. Moreover, they seem to better agree with the present prediction from either of our effective interface equations, $\lambda_m \propto l_D^{1/2}$, than with the linear behavior argued for in [40].

Another important experimental feature is the relation between λ_m and C_a . From Eq. (20) we know that

$\Omega = (1 - t_c)/C_a$; then, $d_0 = \Omega\Gamma = \Omega\gamma/RT$, so that the characteristic length scale λ_m will be proportional to $C_a^{-1/2}$. Thus, one would expect the branches to be narrower as we increase the initial concentration, consistent with the patterns obtained by Lèger *et al.*

We will try also to interpret the ECD experiments of Schiardi *et al.* [18]. They have measured the interface global width considering that the topmost heights of the branches provide a well-defined front. Thus, the time evolution of the global width, or roughness, presents three different well-defined regimes: A short initial transient, which cannot be accurately characterized by any power law due to the lack of measured points, is followed by an unstable transient. We consider the system unstable in the sense that the average interface velocity is *not* a constant, but rather grows with time. Finally, the system reaches a regime characterized by exponent values that are compatible with those of the KPZ equation, while the aggregate grows at a constant velocity. These regimes again resemble qualitatively the behavior expected for the noisy KS equation (57).

Moreover, we can check whether the order of magnitude of the experimental parameters is compatible with our predictions. First, we estimate k_m from the mean width of the branches within the unstable regime. This width is about 0.05 mm [18]; hence, $k_m \approx 1.3 \times 10^3 \text{ cm}^{-1}$. Besides this, the mean aggregate velocity at long times is $V \approx 2 \times 10^{-4} \text{ cm s}^{-1}$ and the diffusion coefficient is $D \approx 10^{-5} \text{ cm}^2 \text{ s}^{-1}$, so that the diffusion length is about $l_D = D/V \approx 0.05 \text{ cm}$. These magnitudes allow us to calculate the capillarity length $d_0 = 1/2l_D k_m^2 \approx 5 \times 10^{-6} \text{ cm}$ (which is of the same order as we considered in our approximations above and much smaller than the diffusion length). Furthermore, the instability appears at times of order $1/\omega_m$. In the experiment this time is about 6 min. Thus, $\omega_m \approx 3 \times 10^{-3} \text{ s}^{-1}$. Finally, as $\omega_m = k_D l_D k_m^2 / 2$, then $k_D \approx 6 \times 10^{-8} \text{ cm s}^{-1} \ll V$, which provides a consistency criterion for the validity of our approximations and of our predictions.

As a final example, let us perform some comparisons with the mentioned experiments of Pastor and Rubio [52,69]. At short times, they obtain compact aggregates with exponent values [52] $\alpha = 1.3 \pm 0.2$, $\alpha_{loc} = 0.9 \pm 0.1$, $z = 3.2 \pm 0.3$, and $\beta = 0.4 \pm 0.08$. This means that the interface is superrough ($\alpha > 1$). After this superrough regime, the aggregate becomes unstable and the dispersion relation has the MS form. The fact that the aggregates are compact (and not ramified) seems to show that surface diffusion is an important growth mechanism in these experiments (which is also consistent with the small value of the velocity, $V \approx 4 \text{ } \mu\text{m/min}$). Consequently, we can use Eq. (58) with an additional surface diffusion contribution $[-Bk^4 \zeta_k(t)]$ to understand the behavior of the experiments. We choose the parameters $\nu = 0.25$, $K = \Pi_0 = 1$, and $\lambda = \Pi_2 = 0$ (because the velocity is small and we are only interested in the short-time regime) for several positive values of B in order to determine the influence of surface diffusion in the growth exponents. Other parameters only change the characteristic length and time scales of the experiment. The exponents thus obtained numerically—e.g., for $B = 0.75$ —are $\beta \approx 0.39 \pm 0.02$ and $\alpha \approx 1.3 \pm 0.1$, which are (within error bars) equal to the experimental ones. Note that,

since the equation becomes linear ($\lambda=0$) for this parameter set, already power counting shows that the early-time regime before the onset of the morphological instability is dominated by the stabilizing surface diffusion term. Thus, the exponents we obtain are compatible with those of the linear molecular beam epitaxy model ($\beta=3/8$ and $\alpha=3/2$) [14], as expected from the analogous noisy KS case [23]. As pointed out above, this superrough regime is followed by an unstable transient characterized by the MS dispersion relation, as has been also observed in other ECD experiments by de Bruyn [50], and Kahanda *et al.* [51].

More recently, additional ECD experiments have been reported under galvanostatic conditions. E.g., in Ref. [6] three growth regimes can be distinguished: a first one at short times, in which a Mullins-Sekerka-like instability is reported, is followed by a regime in which anomalous scaling (namely, the roughness exponents measured from the global and local surface widths differ, $\alpha \neq \alpha_{loc}$) [15,63,64] takes place, and finally at long times ordinary Family-Vicsek scaling [14] is recovered. Similar transitions to and from anomalous scaling behavior have been also reported in Ref. [8]. Our present theory does not predict the anomalous scaling regimes reported by these authors. This may be due to the small slope condition employed in the derivation of Eqs. (58) and (57). However, we want to emphasize two points in this respect: (i) In Ref. [8] the authors report a transition from rough interface behavior to mound formation. These mounds can be obtained by numerical integration of Eq. (58) in 2+1 dimensions [70]. (ii) As we will show in the next section, the theory is in good agreement with a discrete model of growth in which anomalous scaling is clearly reproduced. Hopefully, a numerical integration of the full moving-boundary problem (42) would capture the anomalous scaling regime, and this will be the subject of further work.

B. Discrete models

As mentioned above, k_D is related to the sticking probability through Eq. (5). This probability acts as a noise reduction parameter [71] in discrete growth models, as was shown, e.g., in [72–74] for the multiparticle-biased diffusion-limited aggregation (MBDLA) model, used to study ECD growth. In particular, the MBDLA model has been seen to describe quantitatively the morphologies obtained in [18]. In the MBDLA model, by reducing the sticking probability, the asymptotic KPZ scaling is indeed more readily achieved, reducing the importance of pre-asymptotic unstable transients, as illustrated by Fig. 8 of [74]. Hence, noise reduction is not a mere computational tool for discrete models, but rather it can be intimately connected with the surface kinetics via Eqs. (5) and (26).

The MBDLA model with surface diffusion also predicts the existence of a characteristic branch width. This is shown in Fig. 8 in which the power spectral density is plotted and compared with the one obtained from the noisy KS equation, proving the equivalence between both descriptions of ECD. These results are reinforced by the fact that, as shown in Ref. [74], the cation concentration obeys Eq. (44) and the branch width dependence on the cation concentration is consistent

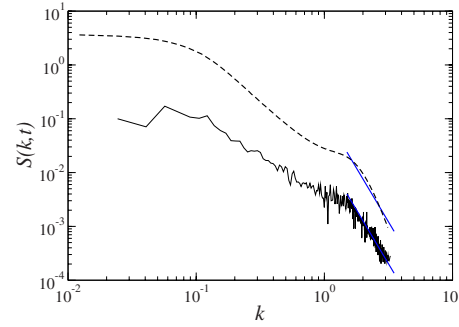


FIG. 8. (Color online) Power spectrum obtained from MBDLA simulations (solid line) with $r=0.5$, $p=0.5$, $s=1$, $c=1$ (taken from Fig. 15 in [74], by permission), and Eq. (57) with $\nu=1$, $K=1/4$, $\lambda=40$, $\Pi_0=10^{-2}$, and $L=512$ (dashed line), averaged over 10^5 realizations. For the sake of clarity, the latter has been vertically offset. Straight blue lines are guides to the eye having slope -4 . Axes are in arbitrary units.

with the relation $\lambda_m \propto C_a^{-1/2}$. Moreover, in simulations of the MBDLA model, an unstable transient was found before the KPZ scaling regime, being characterized by intrinsic anomalous scaling, as recently observed in the experimental works by Huo and Schwarzacher [75,76]. As mentioned, probably the absence of such an anomalous scaling transient in our continuum model is related to the small-slope approximation and we expect to retrieve it from a numerical integration of the full moving-boundary problem.

VI. CONCLUSIONS

In this paper we have provided a derivation of stochastic interface equations from the basic constitutive laws that apply to growth system in which aggregating units are subject to diffusive transport and attach only after (possibly) finite reaction kinetics. Our derivation seems to be new for this class of systems and allows us to relate the coefficients in the effective interface equation with physical parameters, like the sticking parameter, physical surface tension, size of aggregating units, etc. We have seen that the shape of the equation describing the time evolution of the aggregate interface changes as a function of the sticking probability. For very high interface kinetics nonlocal shadowing effects occur, while for finite kinetics nonlocal shadowing yields to morphological instabilities of a local nature. Thus, qualitatively the behavior of the system for generic parameter conditions roughly consists of an initial transient associated with morphological instabilities in which typical length scales are selected (thus breaking scale invariance), which is followed by a late-time regime in which the interface displays kinetic roughening. However, the universality class of the latter differs, being of the KPZ class only for slow attachment kinetics, while it becomes of a different non-KPZ type for fast attachment, as predicted by the interface equation we obtain in the latter condition. While in previous reports [15,17,20] we have interpreted the long unstable transients as a potential cause for the experimental difficulty in observing KPZ scaling, our present results go one step further in the sense that for fast attachment conditions we do not even expect KPZ

universality in the asymptotic state, due to the irrelevance of the KPZ nonlinearity as compared with the $|k|\zeta_k(t)$ term in Eq. (58). Recall that, as pointed out when discussing Eq. (50), the behavior obtained for the $k_D \rightarrow \infty$ limit applies also to finite values of the kinetic coefficient, provided they are much larger than the average growth velocity. Thus, it is actually the ratio between k_D and V , rather than their magnitudes, that controls the relevance of the different processes taking place at the surface.

Comparison of our continuum model with experiments and discrete models seem to support the above conclusions. Nevertheless, our results are in principle constrained by a small-slope approximation. In view (especially under fast kinetics conditions) of the large roughness exponent values that characterize the long-time interfaces as described by our effective interface equations, it is natural to question whether the same scenario holds for the full (stochastic) moving-boundary problem. Moreover, our small-slope equations do not account for anomalous scaling, which is otherwise seen in experiments and in the MBDLA model, so that integration of the complete system (25)–(28) seems indeed in order. Technically, systems of this type pose severe difficulties even to numerical simulations (mostly related to front tracking in the face of overhang formation). Thus, one needs to rephrase the original continuum description (25)–(28) into an equivalent formulation that is more amenable to efficient numerical simulation, such as, e.g., a phase-field model [77]. We are currently pursuing such a type of approach and expect to report on it soon.

ACKNOWLEDGMENTS

This work has been partially supported by UC3M/CAM (Spain) Grant No. UC3M-FI-05-007, by CAM (Spain) Grant No. S-0505/ESP-0158, and by MEC (Spain), through Grants No. FIS2006-12253-C06-01 and No. FIS2006-12253-C06-06, and the FPU program (M.N.).

APPENDIX A: THE GREEN'S FUNCTION TECHNIQUE

This technique has been used in other similar problems, such as solidification [41] or epitaxial growth on vicinal surfaces [42], and is based on the use of the Green's theorem [44] to transform an integral extended over a certain domain [in our case, say, the region between the electrodes (see Fig. 9) to an integral that is evaluated precisely at the moving boundary (the aggregate surface)].

Let us consider that the distance separating the electrodes and the lateral size of the system are both infinite, so that the only part of the dashed line in Fig. 9 whose contribution is nonvanishing is the aggregate surface. The Green's function related to Eq. (25) is the solution of

$$\left(\frac{\partial}{\partial t'} + D\nabla'^2 - V\frac{\partial}{\partial z'} \right) G(\mathbf{r} - \mathbf{r}', t - t') = -\delta(\mathbf{r} - \mathbf{r}')\delta(t - t'), \quad (\text{A1})$$

where we have made a change of coordinates to a frame of reference moving with the average growth velocity V . To evaluate G , we use its Fourier transform

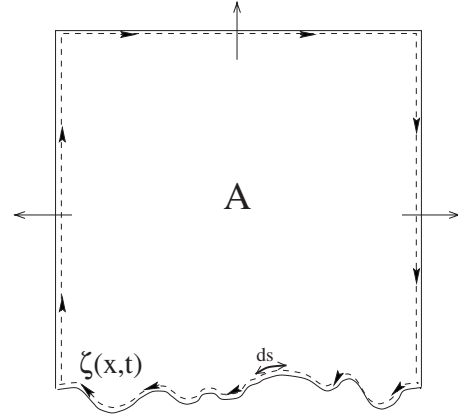


FIG. 9. Integration domain A and its boundary (solid line) used in Green's theorem. The infinitesimal arclength along the moving boundary $\zeta(x, t)$ is given by ds .

$$G(\mathbf{r} - \mathbf{r}', t - t') = \frac{1}{(2\pi)^3} \int d\omega e^{i\omega(t-t')} \int d^2\mathbf{k} e^{i\mathbf{k}\cdot(\mathbf{r}-\mathbf{r}')} G_{\mathbf{k}\omega}, \quad (\text{A2})$$

where $\mathbf{r} = x\hat{\mathbf{x}} + z\hat{\mathbf{z}}$ and $\mathbf{k} = k_x\hat{\mathbf{x}} + k_z\hat{\mathbf{z}}$. Hence, Eq. (A1) becomes

$$G_{\mathbf{k}\omega} = \frac{1}{Dk^2 + i\omega - iVk_z}, \quad (\text{A3})$$

with $k^2 = k_x^2 + k_z^2$. Therefore, integrating Eq. (A2) we find

$$G(\mathbf{r} - \mathbf{r}', t - t') = \frac{\Theta(t - t')}{4\pi D(t - t')} \exp \left[-\frac{(x - x')^2}{4D(t - t')} - \frac{[z - z' + V(t - t')]^2}{4D(t - t')} \right], \quad (\text{A4})$$

$\Theta(t - t')$ being the Heaviside step function. In the following, we will use for brevity $\tau \equiv t - t'$. It can be straightforwardly seen that the following relations are satisfied:

$$\lim_{\tau \rightarrow 0^+} G(\mathbf{r} - \mathbf{r}'; \tau) = \delta(\mathbf{r} - \mathbf{r}'), \quad (\text{A5})$$

$$\lim_{\tau \rightarrow -\infty} G(\mathbf{r} - \mathbf{r}'; \tau) = 0, \quad (\text{A6})$$

$$\int_{-\infty}^t dt' \int_{-\infty}^{\infty} dx' G = \begin{cases} \exp[-(z - z')V/D]/V & \text{if } z > z', \\ 1/V & \text{if } z < z'. \end{cases} \quad (\text{A7})$$

We can now rewrite Eq. (25) in terms of the variables \mathbf{r}' and t' ,

$$\left(\frac{\partial}{\partial t'} - D\nabla'^2 - V\frac{\partial}{\partial z'} \right) c' = -\nabla' \cdot \mathbf{q}'. \quad (\text{A8})$$

Adding Eq. (A8) multiplied by $G(\mathbf{r} - \mathbf{r}', t - t')$ to Eq. (A1) multiplied by $c' \equiv c(x', z'; t')$ and integrating t' in $(-\infty, t - \epsilon]$ and \mathbf{r}' in the set $A = (-\infty, \infty) \times [\zeta(x', t'), \infty)$ (see Fig. 9),

$$\int_{-\infty}^{t-\epsilon} dt' \int_A d^2\mathbf{r}' \frac{\partial}{\partial t'}(c'G) - V \int_{-\infty}^{t-\epsilon} dt' \int_A d^2\mathbf{r}' \frac{\partial}{\partial z'}(c'G) + D \int_{-\infty}^{t-\epsilon} dt' \int_A d^2\mathbf{r}' (c'\nabla'^2 G - G\nabla'^2 c') = - \int_{-\infty}^{t-\epsilon} dt' \int_A d^2\mathbf{r}' G \nabla' \cdot \mathbf{q}'. \quad (\text{A9})$$

The first term on the left-hand side can be easily evaluated with the use of Eqs. (A5) and (A6). Thus,

$$\lim_{\epsilon \rightarrow 0} \int_{-\infty}^{t-\epsilon} dt' \int_A d^2\mathbf{r}' \frac{\partial}{\partial t'}(c'G) = c(\mathbf{r}; t) + \int_{-\infty}^t dt' \int_{-\infty}^{\infty} dx' \frac{\partial \zeta'}{\partial t'} [c'G]_{z'=\zeta'}, \quad (\text{A10})$$

where ζ' stand for $\zeta(x', t')$. Analogously, we can integrate the second term on the left-hand side of Eq. (A9), using (A7):

$$\lim_{\epsilon \rightarrow 0} -V \int_{-\infty}^{t-\epsilon} dt' \int_A d^2\mathbf{r}' \frac{\partial}{\partial z'}(c'G) = -c_a + V \int_{-\infty}^t dt' \int_{-\infty}^{\infty} dx' [c'G]_{z'=\zeta'}. \quad (\text{A11})$$

Finally, using the identity $c'\nabla'^2 G - G\nabla'^2 c' = \nabla' \cdot (c'\nabla' G - G\nabla' c')$ and applying Green's theorem on the domain A , we get

$$\lim_{\epsilon \rightarrow 0} D \int_{-\infty}^{t-\epsilon} dt' \int_A d^2\mathbf{r}' (c'\nabla'^2 G - G\nabla'^2 c') = -D \int_{-\infty}^t dt' \int_{\zeta'} ds' \left(c' \frac{\partial G}{\partial n'} - G \frac{\partial c'}{\partial n'} \right), \quad (\text{A12})$$

ds' being the arclength (see Fig. 9), from which we obtain the integro-differential equation

$$c(\mathbf{r}, t) = c_a - \int_{-\infty}^t dt' \left[\int_{-\infty}^{\infty} dx' \left(V + \frac{\partial \zeta'}{\partial t'} \right) c'G - D \int_{\zeta'} ds' \left(c' \frac{\partial G'}{\partial n'} - G \frac{\partial (c'_0 + c'_1)}{\partial n'} \right) \right]_{z'=\zeta'} - \sigma(\mathbf{r}, t), \quad (\text{A13})$$

where

$$\sigma(\mathbf{r}, t) = \int_{-\infty}^t dt' \int_{-\infty}^{\infty} dx' \int_{\zeta'} dz' G \nabla' \cdot \mathbf{q}' \quad (\text{A14})$$

is a term related to the diffusion noise.

As we seek to determine c everywhere, we need to know its value at the boundary. Considering the limit in which \mathbf{r} belongs to that boundary (hereafter, we will denote it as \mathbf{r}_b), the term $\partial G / \partial n'$ in Eq. (A13) is singular. Fortunately, this singularity is integrable, as a result of which we obtain an additional term as [42]

$$\int_{\mathbf{r} \in \zeta} c' \frac{\partial G}{\partial n'} \rightarrow \frac{c}{2D} + \int_{\mathbf{r}_b \in \zeta} c' \frac{\partial G}{\partial n'}. \quad (\text{A15})$$

This leads to Eq. (42) of the main text, where we have omitted the subindex b for notational simplicity.

APPENDIX B: ZERO-ORDER CALCULATION

Writing $c = c_0 + c_1$ in Eq. (42) we get

$$\frac{c_0}{2} + \frac{c_1}{2} = c_a - \int_{-\infty}^t dt' \int_{-\infty}^{\infty} dx' \left[V(c'_0 G + c'_1 G) + \frac{\partial \zeta'}{\partial t'} c'_0 G - D \left((c'_0 + c'_1) \frac{\partial G}{\partial n'} - G \frac{\partial (c'_0 + c'_1)}{\partial n'} \right) \right]_{z'=\zeta'} - \sigma(\mathbf{r}, t). \quad (\text{B1})$$

Note that, at this order, $ds' = \sqrt{1 + (\partial_x \zeta)^2} dx' \simeq dx'$. We also linearly expand G , so that

$$G(\mathbf{r} - \mathbf{r}', t - t') \simeq \left(1 - V \frac{\zeta - \zeta'}{2D} \right) G^0, \quad (\text{B2})$$

where

$$G^0 = \frac{\Theta(\tau)}{4\pi D \tau} \exp \left[-\frac{(x - x')^2}{4D\tau} - \frac{V^2 \tau}{4D} \right]. \quad (\text{B3})$$

In order to determine the concentration at the boundary, we must write our main equation in terms of c_0 and c_1 . Then, with the use of the boundary condition (26) we find

$$D \frac{\partial (c_0 + c_1)}{\partial n} = k_D (c_0 + c_1 - c_{eq}^0 + \Gamma \partial_x^2 \zeta + \chi) + \mathbf{q} \cdot \mathbf{n}. \quad (\text{B4})$$

Finally, putting Eqs. (B2) and (B4) into (B1) we find

$$\begin{aligned} \frac{c_0}{2} + \frac{c_1}{2} = c_a + \int \int dt' dx' & \left[\left(-c_0 \frac{\partial \zeta'}{\partial t'} - (k_D + V/2)(c'_0 + c'_1) \right. \right. \\ & + k_D V \frac{c'_0}{2D} (\zeta - \zeta') + k_D c_{eq}^0 \left(1 - \frac{\zeta - \zeta'}{2D} V \right) - \Gamma k_D \zeta'_{x'x'} \\ & \left. \left. + c_0 \frac{\zeta - \zeta'}{2} \left(\frac{V^2}{2D} + \frac{1}{\tau} \right) - c_0 \frac{(x - x') \partial_{x'} \zeta'}{2\tau} \right) G^0 \right]_{z'=\zeta'} \end{aligned}$$

$$- \tilde{\sigma}(\mathbf{r}, t), \quad (\text{B5})$$

with a new noise term

$$\begin{aligned} \tilde{\sigma}(\mathbf{r}, t) = & \int_{-\infty}^t dt' \int_{-\infty}^{\infty} dx' \left[(k_D \chi' + \mathbf{q}' \cdot \mathbf{n}') G^0 \right. \\ & \left. + \int_{\zeta'}^{\infty} dz' G^0 \nabla' \cdot \mathbf{q}' \right]. \end{aligned} \quad (\text{B6})$$

Despite the apparent complexity of these new equations, Eq. (B1) is linear so that Fourier transforming it we get the following algebraic equation which relates all the zeroth-order terms:

$$\frac{c_{k\omega}^0}{2} = \left(c_a + \frac{k_D c_{eq}^0}{V} \right) \delta(k) \delta(\omega) - \left(\frac{V}{2} + k_D \right) c_{k\omega}^0 G_{k\omega}^0, \quad (\text{B7})$$

$c_{k\omega}^0$ being the Fourier transformation of c_0 and

$$G_{k\omega}^0 = [4D\omega i + 4D^2k^2 + V^2]^{-1/2}, \quad (\text{B8})$$

which can be easily inverted, yielding Eq. (43).

APPENDIX C: FIRST-ORDER CALCULATION

From the results obtained in Appendixes A and B we can find an evolution equation which relates $c_{k\omega}^1$ and $\zeta_{k\omega}$. Thus,

$$\begin{aligned} \frac{c_{k\omega}^1}{2} = & \left[-i\omega c_0 - (k_D + V/2) \frac{c_{k\omega}^1}{\zeta_{k\omega}} \right. \\ & + \frac{1}{2D} (k_D c_0 - k_D c_{eq}^0) \left(\frac{1}{G_{k\omega}^0} - V \right) + \Gamma k_D k^2 \\ & \left. + \frac{c_0}{4D} \left(\frac{1}{(G_{k\omega}^0)^2} - V^2 \right) - \frac{c_0}{2} D k^2 \right] G_{k\omega}^0 \zeta_{k\omega} - G_{k\omega}^0 \tilde{\sigma}_{k\omega}, \end{aligned} \quad (\text{C1})$$

$\tilde{\sigma}_{k\omega}$ being the Fourier transformation of $\tilde{\sigma}(\mathbf{r}, t)$; hence,

$$\begin{aligned} c_{k\omega}^1 \left(\frac{1}{2G_{k\omega}^0} + \frac{V}{2} + k_D \right) = & \left[\frac{V}{\Omega D} \left(\frac{1}{2G_{k\omega}^0} - \frac{V}{2} \right) + k_D \Gamma k^2 \right] \zeta_{k\omega} \\ & - \tilde{\sigma}_{k\omega}. \end{aligned} \quad (\text{C2})$$

This equation has two unknowns; hence, in order to solve it, we also need to expand Eq. (27) in powers of c_1 and ζ . Thus,

$$c_{k\omega}^1 = \left(\frac{i\omega}{\Omega k_D} + \Gamma k^2 + \frac{B}{k_D} k^4 \right) \zeta_{k\omega} - \chi_{k\omega} + \frac{ik}{k_D} p_{k\omega}. \quad (\text{C3})$$

Combining both Eqs. (C2) and (C3), we find

$$\mathcal{T}_{k\omega} \zeta_{k\omega} = \beta_{k\omega}, \quad (\text{C4})$$

with

$$\begin{aligned} \mathcal{T}_{k\omega} = & \left(\frac{1}{2G_{k\omega}^0} + \frac{V}{2} + k_D \right) \left(\frac{i\omega}{\Omega k_D} + \Gamma k^2 + \frac{B}{k_D} k^4 \right) \\ & - \frac{V}{\Omega D} \left(\frac{1}{2G_{k\omega}^0} - \frac{V}{2} \right) - k_D \Gamma k^2. \end{aligned} \quad (\text{C5})$$

The new noise term $\beta_{k\omega}$ is the projection of all the noise terms onto the boundary and is given by

$$\begin{aligned} \beta_{k\omega} = & \left(\frac{1}{2G_{k\omega}^0} + \frac{V}{2} + k_D \right) \left(\chi_{k\omega} - \frac{ik}{k_D} p_{k\omega} \right) - \tilde{\sigma}_{k\omega} \\ = & D \Lambda_{k\omega}^{(+)} \chi_{k\omega} - \frac{ik}{k_D} p_{k\omega} (D \Lambda_{k\omega}^{(+)} + k_D) + \int_0^{\infty} dz' (ik q_{k\omega}^x \\ & + q_{k\omega}^z \Lambda_{k\omega}^{(-)}) \exp(-\Lambda_{k\omega}^{(-)} z'), \end{aligned} \quad (\text{C6})$$

where

$$\Lambda_{k\omega}^{(\pm)} = \frac{1}{2DG_{k\omega}^0} \pm \frac{V}{2D}. \quad (\text{C7})$$

These equations allow us to calculate the noise correlations (in Fourier space)

$$\begin{aligned} \langle \beta_{k\omega} \beta_{k'\omega'} \rangle = & \left[\frac{2D^2 c_0}{k_D} |\Lambda_{k\omega}^{(+)}|^2 + 2D c_0 \left(\frac{k^2 + |\Lambda_{k\omega}^{(-)}|^2}{2\text{Re}(\Lambda_{k\omega}^{(-)})} \right) \right. \\ & \left. + 2D_s \nu \frac{k^2}{k_D^2} [D^2 |\Lambda_{k\omega}^{(+)}|^2 + k_D^2 + 2D k_D \text{Re}(\Lambda_{k\omega}^{(+)})] \right] \\ & \times \delta(k + k') \delta(\omega + \omega'). \end{aligned} \quad (\text{C8})$$

Note that, in principle, Eq. (C4) provides us with all the information of the system at linear order—namely, the power spectrum of ζ (by evaluating $\mathcal{T}_{k\omega}^{-1}$ and then integrating out the temporal frequency ω) or the height-height correlations (integrating out the spatial frequency k).

In order to gain insight into the implications of this expansion in ζ , we write Eq. (C4) as the Fourier transformation of a Langevin equation for the interface height,

$$[i\omega - \omega_k] \zeta_{k\omega} = \eta_{k\omega}, \quad (\text{C9})$$

ω_k being a function of k , which we must specify from $\mathcal{T}_{k\omega}$, and $\eta_{k\omega}$ being a noise term related to $\beta_{k\omega}$, which is also δ correlated,

$$\langle \eta_{k\omega} \eta_{k'\omega'} \rangle = \Pi(k) \delta(k + k') \delta(\omega + \omega'), \quad (\text{C10})$$

where Π depends, in general, on k and provides the magnitude of the noise for each Fourier mode; see Sec. IV. Finally, by Fourier transforming the time frequency, we find the linear stochastic partial differential equation (45).

- [1] T. Rosebrugh and W. Miller, *J. Phys. Chem.* **14**, 816 (1910).
- [2] J. Agar, *Discuss. Faraday Soc.* **1**, 26 (1947).
- [3] N. Ibl, Y. Barrada, and G. Trumpler, *Helv. Phys. Acta* **37**, 583 (1954).
- [4] J. Bockris and A. Reddy, *Modern Electrochemistry* (Plenum/Rosetta, New York, 1970).
- [5] A. J. Bard and L. R. Faulkner, *Electrochemical Methods* (John Wiley and Sons, New York, 1980).
- [6] M. C. Lafouresse, P. J. Heard, and W. Schwarzacher, *Phys. Rev. Lett.* **98**, 236101 (2007).
- [7] K. Krug, J. Stettner, and O. M. Magnussen, *Phys. Rev. Lett.* **96**, 246101 (2006).
- [8] A. Osafo-Acquaah, Y. Shapir, and J. Jorne, *J. Electrochem. Soc.* **153**, C535 (2006).
- [9] K. Jensen and W. Kern, *Thin Film Processes II* (Academic, Boston, 1991).
- [10] M. Pelliccione, T. Karabacak, and T.-M. Lu, *Phys. Rev. Lett.* **96**, 146105 (2006).
- [11] W. B. White, K. Rykaczewski, and A. G. Fedorov, *Phys. Rev. Lett.* **97**, 086101 (2006).
- [12] A. Yanguas-Gil, J. Cotrino, A. Barranco, and A. R. González-Elipe, *Phys. Rev. Lett.* **96**, 236101 (2006).
- [13] P. Tabeling, *Introduction to Microfluidics* (Oxford University Press, Oxford, 2005).
- [14] A.-L. Barabási and H. E. Stanley, *Fractal Concepts in Surface Growth* (Cambridge University Press, Cambridge, England, 1995).
- [15] R. Cuerno and L. Vázquez, *Advanced in Condensed Matter and Statistical Physics* (Nova Science, New York, 2004).
- [16] M. Kardar, G. Parisi, and Y.-C. Zhang, *Phys. Rev. Lett.* **56**, 889 (1986).
- [17] R. Cuerno, M. Castro, J. Muñoz García, R. Gago, and L. Vázquez, *Eur. Phys. J. Spec. Top.* **146**, 427 (2007).
- [18] P. L. Schilardi, O. Azzaroni, R. C. Salvarezza, and A. J. Arvia, *Phys. Rev. B* **59**, 4638 (1999).
- [19] F. Ojeda, R. Cuerno, R. Salvarezza, and L. Vázquez, *Phys. Rev. Lett.* **84**, 3125 (2000).
- [20] R. Cuerno and M. Castro, *Phys. Rev. Lett.* **87**, 236103 (2001).
- [21] R. Cuerno and M. Castro, *Physica A* **314**, 192 (2002).
- [22] Y. Kuramoto, *Chemical Oscillation, Waves and Turbulence* (Springer, Heidelberg, 1984).
- [23] R. Cuerno, H. A. Makse, S. Tomassone, S. T. Harrington, and H. E. Stanley, *Phys. Rev. Lett.* **75**, 4464 (1995).
- [24] R. Cuerno and K. B. Lauritsen, *Phys. Rev. E* **52**, 4853 (1995).
- [25] K. Ueno, H. Sakaguchi, and M. Okamura, *Phys. Rev. E* **71**, 046138 (2005).
- [26] C. H. J. V. den Breckel and A. K. Jansen, *J. Cryst. Growth* **43**, 364 (1978).
- [27] B. J. Palmer and R. G. Gordon, *Thin Solid Films* **158**, 313 (1988).
- [28] G. S. Bales, A. C. Redfield, and A. Zangwill, *Phys. Rev. Lett.* **62**, 776 (1989).
- [29] W. W. Mullins, *J. Appl. Phys.* **28**, 333 (1957).
- [30] W. W. Mullins, *J. Appl. Phys.* **30**, 77 (1959).
- [31] K. R. Naqvi, K. J. Mork, and S. Waldenström, *Phys. Rev. Lett.* **49**, 304 (1982).
- [32] Sometimes the system contains also other noncharged molecules that affect only the effective mass transport (i.e., the diffusivities), but not the main evolution equations.
- [33] L.-G. Sundström and F. H. Bark, *Electrochim. Acta* **40**, 599 (1995).
- [34] M. Haataja, D. J. Srolovitz, and A. B. Bocarsly, *J. Electrochem. Soc.* **150**, C699 (2003).
- [35] M. Haataja, D. J. Srolovitz, and A. B. Bocarsly, *J. Electrochem. Soc.* **150**, C708 (2003).
- [36] V. Fleury, M. Rosso, J.-N. Chazalviel, and B. Sapoval, *Phys. Rev. A* **44**, 6693 (1991).
- [37] J.-N. Chazalviel and V. Fleury, *Phys. Rev. E* **54**, 4480 (1996).
- [38] C. Léger, J. Elezgaray, and F. Argoul, *Phys. Rev. E* **58**, 7700 (1998).
- [39] D. Kashchiev and A. Milchev, *Thin Solid Films* **28**, 189 (1975).
- [40] C. Léger, J. Elezgaray, and F. Argoul, *Phys. Rev. E* **61**, 5452 (2000).
- [41] A. Karma, *Phys. Rev. E* **48**, 3441 (1993).
- [42] O. Pierre-Louis and C. Misbah, *Phys. Rev. B* **58**, 2259 (1998).
- [43] L. D. Landau and E. M. Lifshitz, *Theoretical Physics V: Statistical Physics* (Pergamon, Oxford, 1967), Chap. 113.
- [44] R. Haberman, *Applied Partial Differential Equations*, 4th ed. (Prentice-Hall, Englewood Cliffs, NJ, 2004).
- [45] We can find those zeros by writing Eq. (C5) as a third-order polynomial in a new variable $\Lambda_k \equiv \frac{1}{2DG_0} + \frac{V}{2D}$, which is simpler to deal with.
- [46] M. Castro, Ph.D. thesis, Universidad Complutense de Madrid, 2001.
- [47] P. Meakin, *Fractals, Scaling and Growth Far from Equilibrium* (Cambridge University Press, Cambridge, England, 1998).
- [48] W. W. Mullins and R. F. Sekerka, *J. Appl. Phys.* **34**, 323 (1963).
- [49] W. W. Mullins and R. F. Sekerka, *J. Appl. Phys.* **35**, 444 (1964).
- [50] J. R. de Bruyn, *Phys. Rev. E* **53**, R5561 (1996).
- [51] G. L. M. K. S. Kahanda, X.-q. Zou, R. Farrell, and P.-z. Wong, *Phys. Rev. Lett.* **68**, 3741 (1992).
- [52] J. M. Pastor, Ph.D. thesis, Universidad Nacional de Educación a Distancia, 1997.
- [53] D. P. Barkey, R. H. Muller, and C. W. Tobias, *J. Electrochem. Soc.* **136**, 2207 (1989).
- [54] F. Ojeda, R. Cuerno, R. Salvarezza, F. Agulló-Rueda, and L. Vázquez, *Phys. Rev. B* **67**, 245416 (2003).
- [55] J. García-Ojalvo and J. M. Sancho, *Noise in Spatially Extended Systems* (Springer-Verlag, New York, 1999).
- [56] C. Canuto, M. Y. Hussaini, A. Quarteroni, and T. A. Zang, *Spectral Methods in Fluid Dynamics* (Springer-Verlag, New York, 1987).
- [57] A. Giacometti and M. Rossi, *Phys. Rev. E* **62**, 1716 (2000).
- [58] R. Toral (unpublished).
- [59] L. Giada, A. Giacometti, and M. Rossi, *Phys. Rev. E* **65**, 036134 (2002).
- [60] L. Giada, A. Giacometti, and M. Rossi, *Phys. Rev. E* **66**, 019902(E) (2002).
- [61] R. Gallego, M. Castro, and J. M. López, *Phys. Rev. E* **76**, 051121 (2007).
- [62] M. Nicoli, R. Cuerno, and M. Castro (unpublished).
- [63] J. M. López, M. A. Rodríguez, and R. Cuerno, *Phys. Rev. E* **56**, 3993 (1997).
- [64] J. M. López, M. A. Rodríguez, and R. Cuerno, *Physica A* **246**, 329 (1997).
- [65] J. Krug and P. Meakin, *Phys. Rev. Lett.* **66**, 703 (1991).

- [66] C.-P. Chen and J. Jorne, *J. Electrochem. Soc.* **138**, 3305 (1991).
- [67] J. Elezgaray, C. Lèger, and F. Argoul, *J. Electrochem. Soc.* **145**, 2016 (1998).
- [68] C. Lèger, J. Elezgaray, and F. Argoul, *Phys. Rev. Lett.* **78**, 5010 (1997).
- [69] J. M. Pastor and M. A. Rubio, *Phys. Rev. Lett.* **76**, 1848 (1996).
- [70] M. Castro, I. Buijnsters, M. Nicoli, R. Cuerno, and L. Vázquez (unpublished).
- [71] J. Kertész and D. Wolf, *J. Phys. A* **21**, 747 (1988).
- [72] A. Sánchez, M. J. Bernal, and J. M. Riveiro, *Phys. Rev. E* **50**, R2427 (1994).
- [73] M. Castro, R. Cuerno, A. Sánchez, and F. Domínguez-Adame, *Phys. Rev. E* **57**, R2491 (1998).
- [74] M. Castro, R. Cuerno, A. Sánchez, and F. Domínguez-Adame, *Phys. Rev. E* **62**, 161 (2000).
- [75] S. Huo and W. Schwarzacher, *Phys. Rev. Lett.* **86**, 256 (2001).
- [76] W. Schwarzacher and S. Huo, *Phys. Rev. Lett.* **91**, 119601 (2003).
- [77] R. González-Cinca, R. Folch, R. Benítez, L. Ramírez-Piscina, J. Casademunt, and A. Hernández-Machado, *Advanced in Condensed Matter and Statistical Physics* (Nova Science, New York, 2004).